



20

## Abstract

21 Palaeoecological data provide insight into how ecosystems have changed in the past, and,  
22 with the development of new sources of proxy data and statistical methods, they are being  
23 used to address questions around the underlying mechanisms of change, such as biotic-  
24 and climate-ecosystem interactions. However, inferences from palaeoecological data can be  
25 hindered by uncertainties inherent in core-type samples that arise from environmental  
26 processes and observer-introduced error. Environmental processes, core extraction  
27 methods, sub-sampling strategies, laboratory methods, and data processing can potentially  
28 mask 'true' signals in the data. How different sources of uncertainty influence the  
29 inferences drawn from palaeoecological data is rarely assessed, but is critical to the  
30 confidence of our conclusions. To address this concern, we use a virtual ecological  
31 approach to assess the effects of environmental and observer introduced uncertainty to  
32 better understand which of them most influence statistical methods applied to the data.  
33 Quantifying information loss from uncertainty can inform study design before a project is  
34 carried out, and so increase the likelihood of detecting a given signal of interest and make  
35 more robust inferences from statistical analyses of palaeoproxy data. We generate  
36 synthetic 'error-free' core-type samples of pseudoproxies, on which environmental and  
37 observational processes are systematically introduced to impose uncertainties on the  
38 simulated pseudoproxies. The influence of three sources of uncertainty (core mixing, sub-  
39 sampling, and proxy quantification from sub-samples), are assessed for their individual  
40 and combined effects on two statistical methods used to synthesise palaeoecological  
41 records: Fisher Information and principal curves. Increasing sub-sampling intervals has the  
42 most influence on the two statistical methods applied to the pseudoproxy data. When  
43 combined, the interaction between increasing sub-sampling interval, and decreasing the  
44 number of proxies counted per sub-sample has the strongest influence on Fisher  
45 Information and principal curves. Fisher Information and principal curves are not affected  
46 in the same way by introducing uncertainty, with principal curves being less influenced by  
47 simulated proxy counting and sub-sampling of the core. Virtually assessing uncertainties is  
48 a powerful method to better understand the influence that uncertainties introduced at  
49 different parts of the analytical process have on conclusions drawn from palaeoecological  
50 data.

## 51 **1 Introduction**

52 Palaeoecological data extends the temporal extent over which we can investigate  
53 ecosystem change well beyond the observational record (Kosnik and Kowalewski, 2016).  
54 These long-term records are crucial for understanding ecosystem trajectories and climate-  
55 ecosystem interactions, as such dynamics may unfold over centuries or millennia (Jackson,  
56 2007). Many proxies and statistical methods are used to address how ecosystems respond  
57 to environmental and human pressures through time. Palaeoecologists use these data to go  
58 beyond describing past changes in, for example, the relative abundances of species, to  
59 uncover underlying mechanisms of change such as biotic interactions and species-  
60 environment relationships (Williams et al., 2011). However, the inferences drawn from  
61 palaeoecological data may be limited by their uncertainties, such as a paucity of  
62 observations over time and space, environmental degradation of samples, and observer-

63 introduced error. Thus, to make robust inferences from palaeoecological data, such  
 64 uncertainties need to be better understood and quantified. Here, we focus on proxies  
 65 reflecting species community data such as fossil pollen extracted from a core sample and  
 66 quantified on microscope slides.

### 67 **1.1 Uncertainties in palaeoecological data**

68 Palaeoecological data derived from core-type samples are subject to numerous  
 69 uncertainties, including: (i) environmental effects and landscape processes affecting the  
 70 sample before extraction; (ii) the methods used in the field to extract the sample; (iii)  
 71 laboratory techniques applied to extract and quantify data from the core; and (iv)  
 72 quantitative analyses applied to the data (Table 1). Environmental processes and  
 73 observation error can affect the representation of species in the data (e.g., their observed  
 74 relative abundances; Goring et al., 2013). Sub-sampling strategies may alter the  
 75 chronological placement of events (Liu et al., 2012; Parnell et al., 2008). Manipulation of  
 76 data, such as interpolation to satisfy statistical assumptions, can introduce statistical  
 77 artifacts and increase type-I error rates (i.e., a false positive). Such uncertainties affect the  
 78 robustness of statistical results and the inferences we may draw from them.

*Table 1: Sources of uncertainty from pre-sampling natural processes to statistical analyses of data. Uncertainties are not independent across categories and can propagate through the observational process and subsequent analyses.*

Source of Uncertainty	Examples
Physical, chemical and biological processes acting on the core or proxy. Not introduced by the observer.	Hiatuses, catchment erosion, variable sedimentation rates and mixing, bioturbation, changing sources of sediment or peat over time, preservation and taphonomy, occurrence of proxy in sample vs. actual abundance, differential preservation of proxies.
Observer introduced error from sampling collection and protocol.	Core compression during extraction, coring location (within basin or broader geographical context), sample depth/length and replication, core overlap, contamination.
Post-collection methods applied a sample and subsamples.	Contiguous/non-contiguous sub-sampling, sub-sampling resolution/density/thickness, sampling error/noise, proxy selection, taxonomic resolution, count method and proxy specific method error, dating frequency, dating precision and accuracy, observational error in proxy count.
Data processing and interpretation.	Age-depth modelling, radiocarbon calibration, detrending, time-averaging, statistical methods selection, and understanding of proxy responses to environmental drivers.

## 79 1.2 Pseudoproxy experiments and virtual ecology

80 Virtual ecology (VE) can be used to assess the influence of uncertainty on statistical  
81 methods and associated inferences (Zurell et al., 2010). In the VE approach, simulated data  
82 are used as testbeds for recreating, in simulation, observational processes. The synthetic  
83 data provide an ‘error-free’ benchmark against which to assess simulated observational  
84 processes and analytical methods. The underlying concept is that the synthetic data mimic  
85 the statistical properties of empirical data without being subject to the same issues of, for  
86 example, limited grain size or extent (Smerdon, 2012). Similarly, the simulated  
87 observational process aims to recreate the statistical properties of the observer, such as the  
88 chance of observing a species occurring at low abundances. Here, we adopt a VE approach  
89 to (i) assess uncertainties introduced by environmental processes and observer-introduced  
90 error by simulating data analogous to a sediment core-type sample, and (ii) to virtually  
91 recreate environmental processes acting on a core, and the observational methods used to  
92 extract data from the core sample. The VE approach follows the form: generate data →  
93 simulate the observational process → analyse the ‘true’ and ‘observed’ data → assess the  
94 analyses of the observed data against the ‘true’ data. We extend this approach to include  
95 simulated environmental process errors that occur before the observational process. The  
96 steps of our adapted VE approach: data generation, degradation, observation, analysis, and  
97 assessment are described in sections 2.1 through 2.3. Empirical data typically lack an  
98 ‘error-free’ control, and even high-quality empirical data (e.g., highly resolved proxy data  
99 from a laminated lake sediment core) incorporate multiple uncontrollable sources of  
100 uncertainty. Virtual experimentation allows for the effects of sources of uncertainty to be  
101 explored for their individual and interaction effects in a systematic and controlled way  
102 (Smerdon, 2012).

103 The VE approach is similar to pseudoproxy experiments where modified observational  
104 data or pseudoproxies (i.e., simulated proxy data) are used in place of empirical  
105 observations (Mann and Rutherford, 2002) and analysed in the same way as empirical  
106 measurements (Asena et al., 2024). Pseudoproxy experiments originated in climatology  
107 where they are a method of assessing palaeoclimate reconstructions (Bothe et al., 2019;  
108 Christiansen et al., 2009; Mann and Rutherford, 2002); here, we apply the same concepts to  
109 palaeoecological data. We use the term virtual ecology to describe the approach by which  
110 synthetic data are generated, sampled from and analysed in ways comparable to empirical  
111 data (Zurell et al., 2010). While simulated data cannot substitute entirely for reality, they  
112 provide an experimental platform (*sensu* Peck, 2004) with which to understand the  
113 processes that influence the formation and analysis of empirical data.

114 Pseudoproxies have been widely used in climatology (Bothe et al., 2019; Mann and  
115 Rutherford, 2002), but virtually assessing sampling methods and statistical approaches on  
116 palaeoecologically relevant data is less common (although see Asena et al., 2024, Benito et  
117 al., 2020, and Blaauw et al., 2010). The lack of understanding of how uncertainties in  
118 palaeoecological data affect the inferences made from them has raised concern (Blaauw,  
119 2012; Blaauw et al., 2020). We address this knowledge gap by:

- 120 (i) generating multivariate pseudoproxy archives (considered analogous to a  
121 time series of proxy data from a core sample);

- 122 (ii) introducing environmental uncertainty to the pseudoproxy archives via  
123 simulated core mixing;
- 124 (iii) introducing process and observer error by virtually recreating the  
125 observational processes of sub-sampling the core and quantifying proxies  
126 from the sub-samples; and
- 127 (iv) applying two multivariate statistical methods independently, Fisher  
128 Information (FI; Fisher, 1922) and principal curves (PrC; Hastie and Stuetzle,  
129 1989), to analyse the ‘error-free’ and degraded/sub-sampled data.
- 130 (v) feature analysis methods (a dimensional-reduction method that collapses  
131 time-series to a set of metrics) are then applied to the FI and PrCs to quantify  
132 the effect of increasing levels of uncertainty

133 Our overarching aim is to quantify the information loss in palaeoecological analyses from  
134 environmental uncertainties, and process and observer error, and how this influences  
135 statistical analysis and inference using such data. We use FI and PrCs as examples that  
136 capture the underlying drivers of a system in different ways. FI captures shorter-term  
137 variance e.g., those driven by short-term stochastic processes. PrCs, as a method of indirect  
138 gradient analysis, primarily captures the long-term ecosystem trends in the pseudoproxies  
139 resulting from the primary driver in the scenarios. A better understanding of how  
140 individual and combined sources of uncertainty affect statistical results and interpretation  
141 can help inform study design (e.g., determining the number of replicate cores or the sub-  
142 sampling resolution needed to detect a signal of interest) and the confidence in the  
143 statistical results of a study.

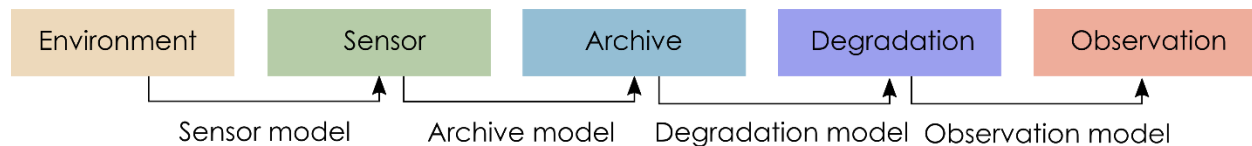
144

## 145 **2 Methods**

### 146 **2.1 Simulating pseudoproxies**

147 Pseudoproxies are simulated using the model described in Asena et al. (2024), following  
148 the proxy system model (PSM) framework (Evans et al., 2013) where a sensor (e.g.,  
149 terrestrial vegetation) responds to environmental drivers and records that response via  
150 proxies (e.g., fossil pollen) counted in an archive such as a lake sediment (in this case a  
151 pseudoproxy record). The model we use follows the conceptual framework of a PSM, but is  
152 not process-based. We adapt the PSM conceptual framework (Evans et al., 2013) to  
153 explicitly include degradation models that describe archive-altering processes before  
154 observations are drawn (Figure 1). Asena et al. (2024) describe the three sub-models that  
155 generate the pseudoproxy data: (i) a driver model representing the environment in which  
156 the archive forms; (ii) a sensor model representing the response of a sensor (e.g.,  
157 terrestrial vegetation) to the environment; and (iii) an archive model that represents how  
158 the response of the sensor is recorded (e.g., as fossil pollen) in a medium such as a  
159 sediment core.

160



161

162 *Figure 1: Adapted Proxy System Model framework (Evans et al., 2013) describing the process*  
 163 *by which environmental drivers act on a sensor, which records its response in an archive, from*  
 164 *which observations are drawn. We have included degradation models to describe processes*  
 165 *acting on the archive before observations are drawn.*

166 ‘Error-free’ pseudo proxies are simulated - in the environment, sensor, and archive sub-  
 167 models (Figure 1). The model consists of four components: (i) environmental driver change  
 168 over time (*environment*); (ii) species’ niches with respect to the driving environment (the  
 169 *sensor* response); (iii) pseudoproxy abundances recording the response to driver change in  
 170 an archive (*archive* record); and (iv) a representation of the formation of the core (*archive*  
 171 characteristics such as core length and accumulation rate). In summary, the model  
 172 generates archives of pseudoproxies consisting of 200 potential species representing a  
 173 palaeoecological record free from the process and observer error associated with empirical  
 174 data. Pseudoproxy abundances are a response to extrinsic and dynamic environmental  
 175 drivers with intrinsic variability from disturbance events, introduction to the population  
 176 via dispersal, and variation in carrying capacity over time. Each species has a tolerance for  
 177 each environmental driver that, together, defines the species niche and determines the  
 178 population growth rate of a species at any given time-step as a function of the  
 179 environmental drivers. If any of the environmental drivers fall outside of a species  
 180 tolerance to that driver, the species will have a negative growth rate and may eventually  
 181 become locally extinct. Species that are tolerant of the current environmental conditions  
 182 can be introduced via dispersal, thus creating a species turnover as conditions change.  
 183 Simulating 200 species covers a wide range of the driver parameter space and allows  
 184 different species assemblages to emerge as driver conditions change. Only a subset of the  
 185 200 species will be presented in the simulated community at any one point in time.

186 Thirty-one replicate models were run for a duration of 5000 time-steps with a burn-in  
 187 period of 500 time-steps applied to allow species to stabilise with respect to the driving  
 188 environment. We aimed for a minimum of 30 replicates to account for model variance, and  
 189 5000 time-steps (c. 5000 years) was sufficiently long to represent ecological turnover in  
 190 the model. The scenario we present here has two environmental drivers: (i) an abrupt  
 191 environmental driver switching between constant conditions; and (ii) a random walk  
 192 driver weighted to 0.15 of the total environmental effect. The magnitude of change in the  
 193 abrupt driver is insufficient to cause a complete species turnover, and generalist species  
 194 survive the shift in extrinsic conditions. The random walk driver may amplify or dampen  
 195 the effects of the abrupt driver, but in general is favourable to most species in the system.  
 196 The parameters for each species are randomised for each replicate model run around the  
 197 same baseline parameters (Table SI2). The results of an additional three scenarios with  
 198 different environmental drivers can be found in the supplementary information. We  
 199 present the abrupt change scenario for two reasons: (i) there are empirical examples of  
 200 such events (e.g., the termination of the Younger Dryas and the Bølling–Allerød warming;  
 201 Williams et al., 2011), and (ii) an abrupt shift in community composition is more likely to

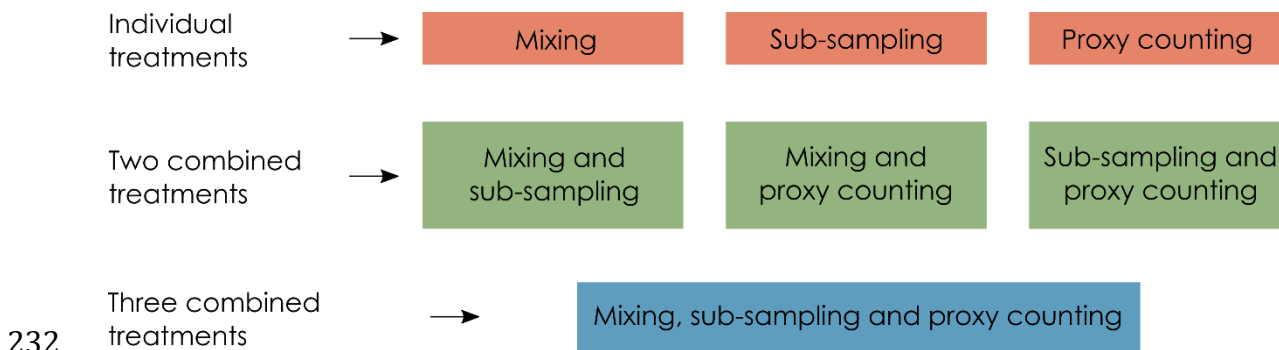
202 be detected by statistical analyses. If the statistical methods we assess perform poorly on  
203 the abrupt scenario, they are unlikely to perform better on more gradual community  
204 turnover.

205

206 Each simulated core is characterised by simulated age, considered to be one year per time-  
207 step, and an increase in depth per time-step. The accumulation rate is represented by a  
208 combination of a linear decrease with time, with a smoothed random walk superimposed  
209 to represent core compression in addition to landscape variability. Variable sedimentation  
210 rates result in a different core length (and accumulation per time-step) for each replicate  
211 simulation and change the number of model time-steps included in a sub-sample of one-  
212 centimetre thickness. Variable change in depth per time-step is calculated as a smoothed  
213 and scaled random walk (similar to Benito et al., 2020) representing landscape changes  
214 and possible hiatuses. A gradual decrease in depth with age can occur from compaction or  
215 compression during extraction (Taranu et al., 2018). The simulated data represent a core-  
216 type sample from which sub-samples are taken, proxies quantified, and data analysed  
217 similar to real-world core samples. The simulated core is used as an ‘error-free’ benchmark  
218 against which methodological and statistical processes are assessed and represents the  
219 complete (and un-degraded) absolute abundance of proxy data.

## 220 2.2 Degradation and sampling of pseudoproxies

221 In this section, we describe the degradation model representing post-depositional  
222 processes affecting the pseudoproxy data (in this case, core mixing), and the observation  
223 models (Figure 1) representing how proxies are quantified from a core sample (here, sub-  
224 sampling and the count method applied to micro-fossils on microscope slides). For details  
225 and visualisations of the degradation models, see Asena et al, (2024). We apply three  
226 treatments to each of the model replicates: mixing (degradation), sub-sampling and proxy  
227 counting (observation), applied at 10 levels each individually and combined (Figure 2).  
228 Together, the degradation and observation models represent process- and observer-  
229 introduced error that affect the data before quantitative analyses are applied. Each of the  
230 31 replicate archives results in 1210 datasets from the ‘error-free’ reference core to the  
231 most uncertain.



232

233 *Figure 2: Each uncertainty (treatment) is applied to the ‘error-free’ pseudoproxy archive to*  
234 *systematically introduce uncertainty individually, and in combination.*

235

236 *2.2.1 Virtual mixing: degradation model*

237 Core mixing is applied as a centrally weighted rolling-average over time-windows of the  
238 archive ranging from unmixed (the 'error-free' benchmark) to a window of 10 time-steps.  
239 Simulated mixing is represented as consistent over time, rather than being a depth-  
240 dependent process such as bioturbation.

241 *2.2.2 Virtual sub-sampling: observation model*

242 An absolute proxy abundance per time-step is generated by the model and is sub-sampled  
243 at regular depth intervals ranging from one to ten centimetres. Each sub-sample has a  
244 thickness of one centimetre; the number of time-steps spanned by the sampled thickness is  
245 determined by the simulated accumulation rate. If the one-centimetre sub-sample covers  
246 multiple time-steps, the proxy abundances in that sub-sample are summed. All sub-sample  
247 treatment data are converted to relative abundances before analysis so that the analyses  
248 are not influenced by excessive values from the summed proxies of multiple time-steps.  
249 When applied in combination with simulated proxy counting, values are converted to  
250 relative abundance after the proxy count treatment.

251 *2.2.3 Virtual proxy count: observation model*

252 The process of counting proxies in a sub-sample (e.g., counting several hundred pollen  
253 grains or diatoms on a microscope slide) is simulated by random sampling from the  
254 absolute proxy abundances with resolutions increasing from 100 to 1000 by 100. The  
255 probability of a proxy occurring in the random sample is based on the abundance of that  
256 proxy. The sample is then converted to relative abundances comparable to empirical proxy  
257 data. The simulated count treatment is applied to the raw, mixed, and sub-sampled data.  
258 Increasing levels of uncertainty in the proxy counting treatment are represented by a  
259 decrease in the proxy count resolution.

260 **2.3 Quantitative analyses**

261 After the application of the degradation and observation models, the pseudoproxy data  
262 span a gradient of uncertainty from the 'error-free' data to the uncertain data that reflect  
263 what we observe from a system. We then apply statistical analyses along this gradient to  
264 determine the influence of each source of uncertainty (the penultimate step of the VE  
265 approach). FI and PrCs are used to analyse each treatment level from each replicate core  
266 (treatment level being the severity of each of the treatments, mixing, sub-sampling and  
267 proxy counting). FI and ordination methods have been suggested as appropriate where  
268 there are an unlimited number of input variables of any data type that do not require *a*  
269 *priori* knowledge of the driving state variables of a system (Roberts et al., 2018). The FI and  
270 PrC produce a large amount of data, so we use feature analysis for time-series (FATs; Nun  
271 et al., 2015) to synthesise them and reduce each time-series to a small number of metrics  
272 (or 'features') that we can compare across treatment levels (detailed below). Each replicate  
273 core results in 1210 FI time-series and PrCs, and by extracting a set of features, the  
274 difference among treatment levels can be calculated as a measure of distance, we use

275 Euclidean distance. The data analysis process is as follows: (i) calculate FI and PrC for each  
276 treatment level; (ii) extract features from the FI and PrC outputs; and (iii) calculate the  
277 distance between the features of each treatment level (Figure 3).

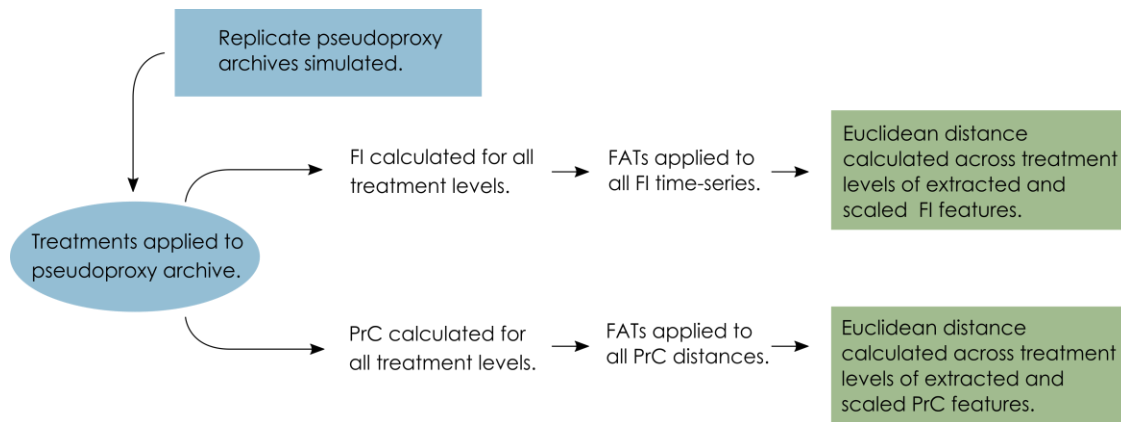


*Figure 3: Conceptual data-flow of the degradation, sampling and analysis process. Treatments of mixing, sub-sampling and proxy counting are applied individually and in combination to the replicate pseudoproxy archives (Figure 2). Fisher information (FI) and principal curves (PrC) are applied separately to each treatment and subsequently analysed using feature analysis for time-series (FATs). Extracted features are scaled and Euclidean distance between each treatment level and the ‘error-free’ reference core is calculated.*

### 278 2.3.1 Fisher Information (FI)

279 Fisher information was developed to quantify information about an unknown parameter  
280 from measurable variables (Fisher, 1922) and has since been used as a measure of  
281 ecosystem stability (Cabezas and Fath, 2002; Eason et al., 2016; Karunanithi et al., 2008;  
282 Mayer et al., 2006). Fisher information has been applied to palaeoecological data, with the  
283 suggestion that it can be used as an indicator of an approaching regime shift, such as a shift  
284 in diatom species’ composition (Spanbauer et al., 2014). Fundamentally, FI evaluates the  
285 probability of detecting different system states over time, or the ‘stability’ of the system;  
286 thus, FI changes with the variance in the system. Pseudoproxies from each replicate core,  
287 and each level of uncertainty, are analysed using FI, using a custom R package (Asena et al.,  
288 2023).

### 289 2.3.2 Principal curves

290 Principal curves can be used to identify the underlying variables (e.g., a steadily changing  
291 variable over time) that describe a system characterised by multiple state variables and can  
292 be considered as a form of non-linear principal components analysis (De’ath, 1999). In  
293 short, a PrC is a one-dimensional curve fit through the ‘middle’ of an  $n$ -dimensional space  
294 (e.g., species composition data; (Hastie and Stuetzle, 1989). The curve represents species  
295 compositions by mapping (or projecting) the sites, e.g., the species’ composition at a given  
296 sample, onto a low-dimensional space, and using similarity or dissimilarity measures to  
297 measure the distance between sites (assessing, for example, the species’ compositional  
298 change through time). The arrangement of sites reflects the composition of species in the

299 reduced dimension space as the distance between sites is proportional to the distance in  
300 species composition (De'ath, 1999). Principal curves can be used as a method of gradient  
301 analysis, the underlying concept being that the species abundances change in a predictable  
302 way along an ecological gradient. Here, we use PrCs to represent change in species  
303 composition over time and as a method of indirect gradient analysis using the distances  
304 along the PrC. Cubic smoothing splines are used to fit the PrC to the data. Hastie and  
305 Stuetzle (1989), De'ath (1999), and Simpson (2012) detail the implementation of PrCs. PrC  
306 analyses were conducted for all replicate pseudoproxy datasets for each level of increasing  
307 uncertainty using the analogue package (Simpson and Oksanen, 2020) in R (R Core Team,  
308 2020).

#### 309 *2.4 Assessing results: Feature analysis for time-series*

310 The final step of the VE approach is to assess the outcomes of the statistical analyses  
311 applied to the degraded and sampled data against the 'error-free' pseudoproxies. To  
312 compare the FI and PrC time-series across treatment levels, we use feature analysis.  
313 Feature analysis is a method of reducing a two-dimensional time-series to a one-  
314 dimensional set of 'features'. Features are metrics that describe a time-series in terms of  
315 summary statistics (e.g., mean and variance), and more complicated descriptors such as  
316 autocorrelation length (Nun et al., 2015). We developed a set of 62 features (Table SI4)  
317 drawing on feature analysis for time-series (Kim et al., 2011; Nun et al., 2015; Richards et  
318 al., 2011; Sokolovsky et al., 2017) and change point analysis (Killick and Eckley, 2014). The  
319 individual and combined degradation and sampling treatments result in 1210 time-series  
320 per replicate, yielding  $31 \times 1210 = 37510$  virtual cores per scenario. Describing the FI time-  
321 series and PrC as a series of features allows comparison between the 1210 treatments by  
322 calculating a distance measure (we use Euclidean distance) between the extracted features  
323 of each treatment level. The feature analysis process is as follows:

- 324 1. Features are extracted from the FI time-series and distances along the PrCs for all  
325 replicate model runs of the 'error-free' archive.
- 326 2. A correlation matrix of the features from the replicate 'error-free' datasets is  
327 constructed, and features with a Pearson's correlation coefficient greater than  $|0.7|$   
328 are excluded sequentially, recalculating the correlation matrix until all highly  
329 correlated features are dropped, starting with the highest correlation coefficient  
330 (Dormann et al., 2007).
- 331 3. The remaining features (with a Pearson's correlation coefficient less than  $|0.7|$ ) are  
332 then calculated for all replicates across all treatment levels, resulting in a number  
333 (ranging between 14-26 per scenario) of single metric features per treatment that  
334 describe the FI time-series and PrC.
- 335 4. The features are scaled (by subtracting the mean of the entire series from each point  
336 and dividing it by the series' standard deviation), and the Euclidean distance is  
337 calculated across treatment levels, resulting in a single distance measure between  
338 the 'error-free' core and each treatment level.
- 339 5. Summaries of the Euclidean distances are calculated for all treatment levels across  
340 replicates, resulting in a single distance measure for each treatment from the 'error-  
341 free' benchmark.

342

### 343 3 Results

#### 344 3.1 Effects of individual sources of uncertainty

345 In the extracted features for FI, sub-sampling causes the largest overall increase in the  
346 median Euclidean distance from the 'error-free' core, followed by proxy counting and then  
347 mixing; however, there is overlap in the confidence envelopes across all three treatments  
348 (Figure 4A). Distance from the 'error-free' core increases consistently with uncertainty in  
349 the mixing treatment, showing a steeper increase in distance across uncertainty compared  
350 with the other two treatments. Between successive treatment levels, proxy counting shows  
351 little increase in the median Euclidean distance as uncertainty increases. In the sub-  
352 sampling treatment, distance increases more in the lower uncertainty levels than in the  
353 higher levels, plateauing somewhat at higher uncertainty (Figure 4A). There is some  
354 variability across the treatment levels resulting from the stochasticity in the underlying  
355 model and simulated observational processes (i.e., proxy counting is a random sampling  
356 process, and sub-sampling is dependent on the variable accumulation rates of the core).

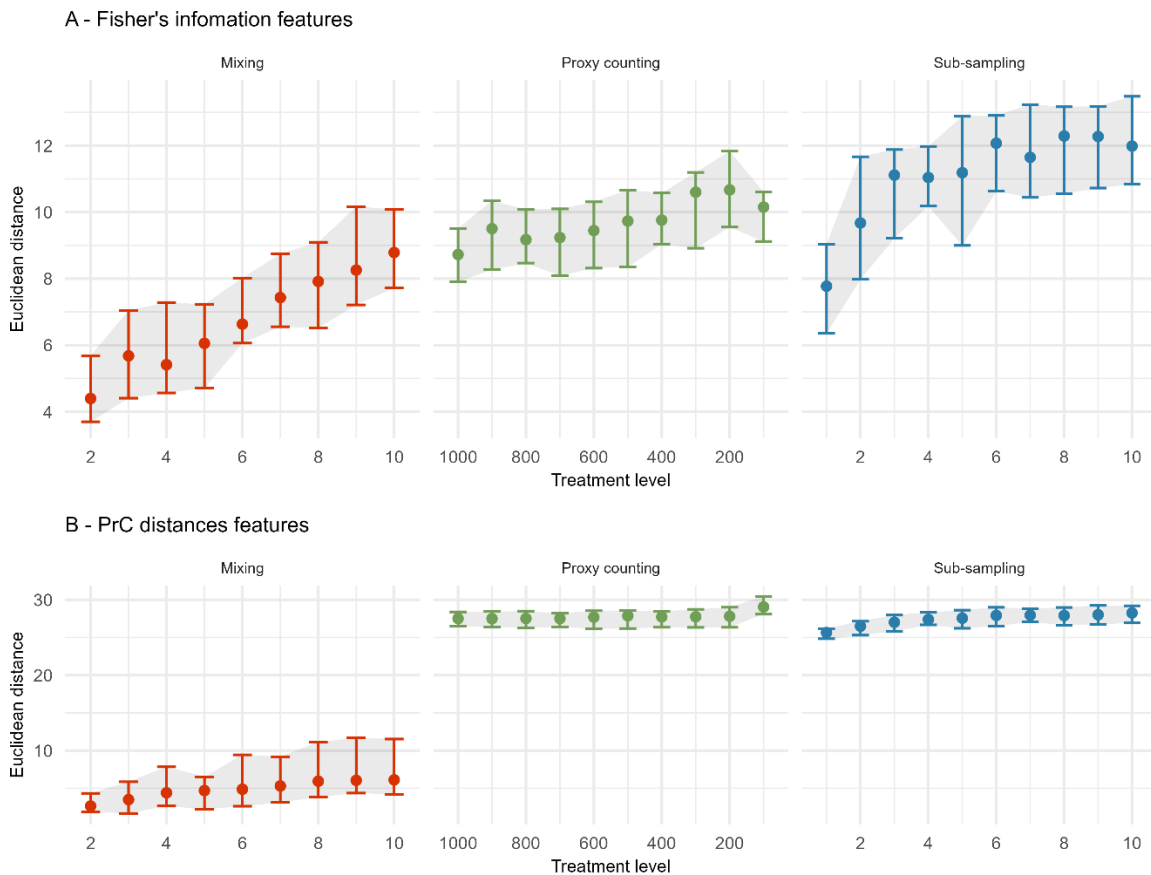


Figure 4: The median (dots), 25th, and 75th quantiles (error-bars and shaded area) of the Euclidean distance from the 'error-free' core of features extracted from the Fisher

*information (A) and PrC distances (B) calculated across replicate simulations. Note the x-axis is organised so uncertainty consistently increases from left-to-right.*

357 For the PrC features, across all scenarios the mixing treatment has the least effect on  
358 median Euclidean distance (Figure 4B). Proxy counting and sub-sampling have overlapping  
359 confidence envelopes, although they are much smaller than those of the mixing treatment.  
360 Proxy counting shows no consistent pattern in median Euclidean distance between  
361 successive treatment levels until the lowest count resolution. Conversely, the sub-sampling  
362 treatment shows an increase in the lower treatment levels, plateauing as sub-sampling  
363 interval increases (Figure 4B).

364

### 365 **3.2 Effects of two combined sources of uncertainty**

366 In the following section, treatments are applied simultaneously to determine which  
367 combinations cause the greatest effect on analyses of the core. The greatest increase in  
368 mean Euclidean distance on the features extracted from FI from the 'error-free' core arises  
369 from the interaction of the sub-sampling and proxy counting uncertainties increasing  
370 together (i.e., along the diagonal; Figure 5A), with a stronger effect from the subsampling  
371 treatment. Mixing combined with sub-sampling or with proxy counting shows no clear  
372 interaction effect as the treatments increase in severity together. The smallest increase in  
373 distance is from the combination of mixing with proxy counting, suggesting that sub-  
374 sampling tends to have the greatest influence of the three treatments (Figure 5A). The  
375 effect of the mixing treatment on the mean Euclidean distance is small when compared to  
376 those of either sub-sampling or proxy counting (Figure 5A). Variability across the surface of  
377 each plot emerges from underlying model stochasticity, random sampling in the simulated  
378 count method, and the variable accumulation rates of the replicate cores.

379

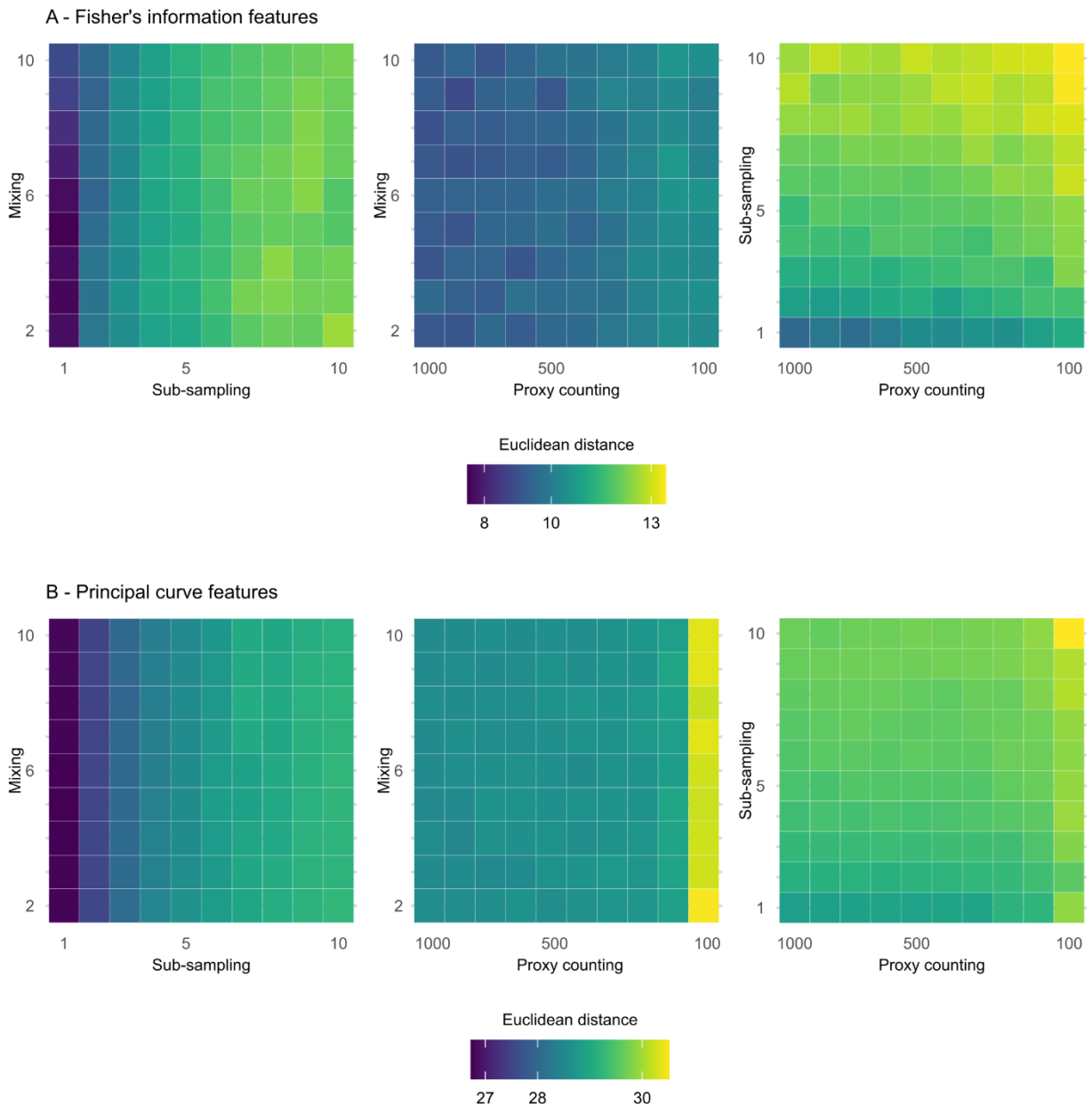


Figure 5: Mean Euclidean distance of features from the 'error-free' core of two treatments combined calculated across replicate simulations for Fisher information (A) and principal curves (B). The mixing axis shows the number of time-steps over which mixing occurs. Along the sub-sampling axis, the frequency of sub-sampling in centimetres is shown, and the proxy counting axis displays count resolutions in number of individuals counted per sample. In the proxy counting treatment, uncertainty increases as count resolution decreases.

380

381

382 In the extracted features from the distances along the PrCs, the combined effects of sub-  
 383 sampling with proxy counting show the largest increase in the mean Euclidean distance of  
 384 all the combined treatments, with a weak interaction effect as proxy count and sub-  
 385 sampling uncertainties increase together (Figure 5B). No interaction effect is visible in  
 386 either the combined treatments of mixing with sub-sampling or mixing with proxy  
 387 counting (Figure 5B).

### 388 3.3 Effects of three combined sources of uncertainty

389 Interaction effects of all three uncertainties applied simultaneously were assessed for the  
 390 extracted FI and PrC features (Figure 6). An interaction effect is visible in the increase of  
 391 mean Euclidean distance as the sub-sampling interval increases (along the x-axis), together  
 392 with proxy counting resolution decreasing (across facets from top left to bottom right);  
 393 however, no clear increase is visible along the mixing axis, indicating little contribution  
 394 from mixing to the interaction of the three treatments (Figure 6). Overall, the greatest  
 395 increase in the mean Euclidean distance among treatments is at the lowest proxy count and  
 396 largest sub-sampling interval.

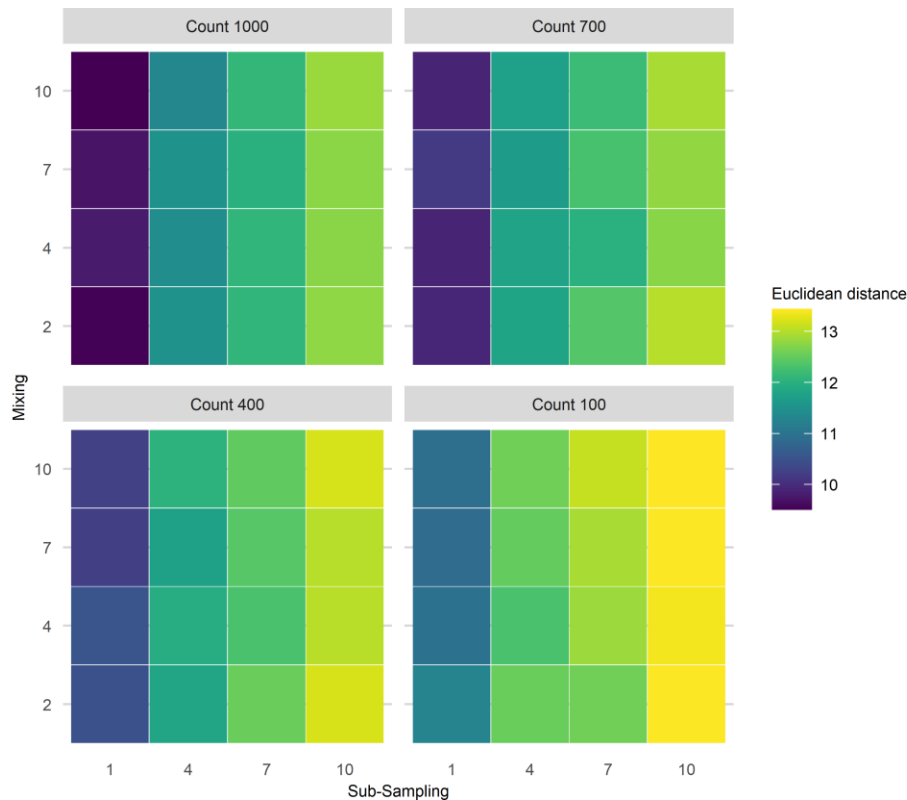


Figure 6: Mean Euclidean distance of Fisher's Information from the 'error-free' core for three treatments applied in combination. To demonstrate the three treatment dimensions, results are displayed such that each plot axis shows mixing (number of time-steps over which mixing occurs) and sub-sampling (frequency in centimetres) treatments, and each facet (sub-plot) is the proxy counting treatment (number of individuals counted in sub-sample). Uncertainty from proxy counting increases from the top left to the bottom right.

397 In the PrC features, applying three treatments in combination does not show a clear three-  
 398 way interaction as uncertainty increases (Figure 7). An increase in mean Euclidean  
 399 distance is visible along the sub-sampling axis (as sub-sampling interval increases), but  
 400 there is little visible effect of the proxy counting treatment (reducing in resolution across  
 401 facets from top left to bottom right) until the lowest resolution. Mixing contributes  
 402 relatively little to the overall increase in mean Euclidean distance showing no visible  
 403 increase along the mixing axis (Figure 7).

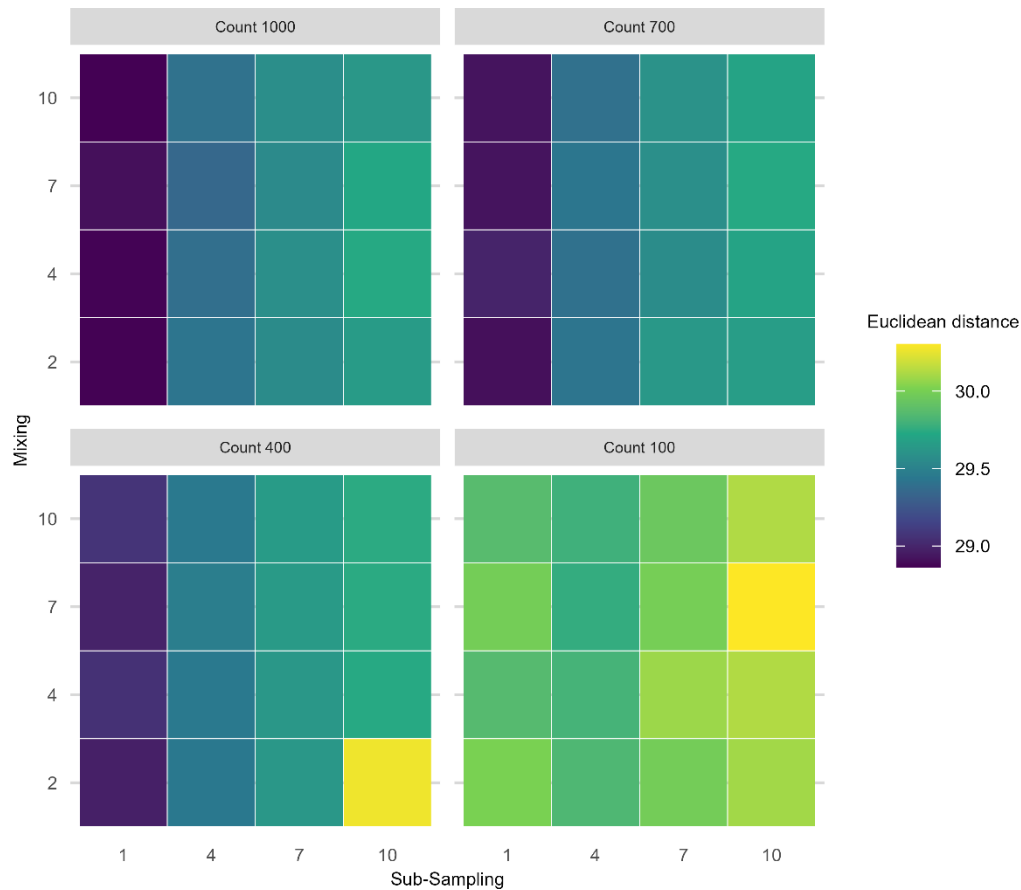


Figure 7: Mean Euclidean distance of the principal curves from the 'error-free' core of all uncertainties increasing in combination. Same plot layout and interpretation as Figure 6.

#### 404 4 Discussion

405 To draw reliable conclusions from palaeoecological data, it is crucial to view our inferences  
 406 in the context of the uncertainties they integrate. Our goal in this paper was to address  
 407 how process and observer error affect statistical methods applied to palaeoecological data  
 408 and the inferences we draw from them. Here, we have assessed some of the uncertainties  
 409 that affect species proxy data. Additionally, uncertainty arises from building chronologies  
 410 (Blaauw et al., 2018; Parnell et al., 2008; Telford et al., 2004) and measuring abiotic system  
 411 variables, such as isotopic records and lake level reconstructions, which carry their own  
 412 uncertainties.

#### 413 4.1 Effects of individual sources of uncertainty

414 Without exception, sub-sampling treatments show the largest effect on the median  
415 Euclidean distances of the FI features (with some overlap in the confidence envelope with  
416 the proxy counting treatment), followed by the proxy counting process. For the PrC  
417 features, both sub-sampling and proxy counting treatments had a similar effect on  
418 Euclidean distance. For both the FI and PrC features, the smallest effect on Euclidean  
419 distance between the 'error-free' and degraded cores came from the simulated mixing  
420 degradation process.

421 Perhaps the most interesting implication of our analyses in the context of empirical ecology  
422 is how the effects of sources of error differ between the two statistical metrics (FI and PrC).  
423 Beyond the initial increase in Euclidean distance in the PrC from the application of proxy  
424 counting and sub-sampling (an unavoidable cost), there was little further effect until the  
425 lowest proxy count and sub-sampling resolutions. Thus, PrCs may be a useful measure of a  
426 system's trajectory for patchy data (e.g., initial analysis of low sub-sampling resolution data  
427 before deciding where to focus sampling effort). For FI, treatment effects have a more  
428 consistent increase in distance from the 'error-free' core with treatment intensity. The  
429 short-term variability captured by FI may provide useful system indicators (*sensu* Eason  
430 and Cabezas, 2012) but may also require high-quality data (e.g., high sub-sampling  
431 resolution and proxy counting) for reliable inferences. The required temporal resolution of  
432 the data is also likely to increase if accumulation rates are slow and species turnover is  
433 rapid. Increased sub-sampling frequency is required in systems that change rapidly  
434 compared with more stable systems where the difference between successive time-steps is  
435 small. Slow accumulation rates mean that a one-centimetre-thick sub-sample integrates  
436 multiple years of ecological change; thus, uncertainty from sub-sampling resolution will  
437 increase if the accumulation rate is slow and ecological change is rapid. An observer may  
438 interpret FI results with the knowledge of which sources of uncertainty, whether  
439 controllable (e.g., sub-sampling and proxy counting resolution) or uncontrollable (e.g.,  
440 mixing and accumulation rates), have the greatest influence. After introducing  
441 uncertainties to the pseudoproxies, the primary patterns, such as long periods of increase  
442 in FI, remain visible and offer a useful depiction of community change.

#### 443 4.2 Effects of combined sources of uncertainty

444 For both FI and PrC, when two treatments are applied in combination, the greatest overall  
445 increase in mean Euclidean distance from the 'error-free' core resulted from sub-sampling  
446 uncertainty in combination with proxy counting uncertainty. For the PrC the maximum  
447 increase in mean Euclidean distance for two simultaneous treatments occurred at the  
448 lowest proxy count resolution in combination with mixing, but such a low proxy count  
449 resolution is unlikely in any empirical study. In our analyses, mixing has relatively little  
450 effect compared with sub-sampling or proxy counting, and the effect tends to be obscured  
451 by other sources of stochasticity (disturbance, dispersal, and temporal changes in carrying  
452 capacity), variable accumulation rates, and randomised sampling of the proxy abundances.  
453 Similarly, when three sources of uncertainty are combined, mixing shows the least effect,  
454 and no apparent interaction with sub-sampling or proxy counting. However, it is worth  
455 noting, that our implementation of mixing is relatively simple in that the effect on the

456 pseudoproxy data is a centrally weighted smoothing. More extreme mixing, and time-  
457 varied mixing effects are likely to show a stronger effect.

458 In the case of FI, the greatest benefit in terms of reducing the distance from the 'error-free'  
459 core came from increasing sub-sampling resolution followed by proxy count resolution.  
460 However, from the standpoint of an observer, increasing the resolution of an FI time-series  
461 may not increase the information content, at least in terms of capturing long-term patterns.  
462 Simple driving environments (e.g., the single driver simulations) are likely to be adequately  
463 represented by FI applied to low-resolution data; however, interpretation of FI from  
464 environments influenced by multiple drivers is potentially challenging without  
465 considerable knowledge of the underlying driving conditions. The benefit of the VE  
466 approach is that it allows us to examine how the underlying dynamics manifest in  
467 multivariate indicators of change, such as FI; however, such near-complete information is  
468 rarely, if ever, available. Ultimately, an observer must base sampling and analysis decisions  
469 on their specific aims. If accurate evaluation of short-term variability is a goal (e.g., for  
470 studies of ecosystem resilience), then dedicating resources to sub-sampling resolution is  
471 likely to be beneficial to analyses such as FI. Reducing observer error, a more controllable  
472 source of error, may help detect a short-term signal of interest if the uncontrollable sources  
473 of error, such as sediment accumulation rates, mixing, and driver variability, are  
474 sufficiently small that the signal remains detectable.

475 PrC shows little increase in distance (after the initial increase from the application of the  
476 treatments) from the 'error-free' reference with combined treatment levels. Thus, as a  
477 representation of compositional change, it may be robust to low-resolution data (e.g.,  
478 infrequent sub-sampling). Short-term changes in abundance (e.g., small disturbances) will  
479 likely become less evident in the PrC; however, our results suggest that overall patterns  
480 seen in a PrC are robust to multiple sources of error. Thus, from the perspective of an  
481 observer, high-resolution data may only be required for PrC to identify short-term  
482 compositional changes, such as perturbations that take a few generations to recover from.

### 483 **4.3 Lessons from virtual ecology for empirical studies**

484 Using virtual ecology to estimate the influence of sources of uncertainty on quantitative  
485 analyses helps us to understand what can be done to mitigate their effects and where to  
486 focus limited resources, such as time spent analysing an individual core. Trade-offs are  
487 inherent in any sampling design. For example, is it more advantageous to focus effort on  
488 spatial coverage by taking multiple cores rather than increasing sub-sampling resolution  
489 on fewer cores? Such questions, of course, depend on the intention of the study and  
490 knowledge of the study site/system (i.e., some knowledge of the uncertainties that will be  
491 encountered, such as landscape changes through time). Virtual ecology allows us to make a  
492 more informed decision about what field and laboratory methods, and quantitative  
493 analyses will be most appropriate given the question of interest. For example, if analysing a  
494 network of core data over a large geographic region, where the observer is interested in the  
495 spatial consistency of the system's trajectory but there are not the resources to extract  
496 highly resolved data from each core, methods such as PrC may be more informative than FI.  
497 Conversely, if an observer is interested in short-term change in a single core (or a region of  
498 particular interest in a core), it may be worth allocating the time to extracting highly

499 resolved data to increase the reliability of analyses sensitive to variance such as FI. PrC and  
500 FI provide different representations of a system's trajectory. Principal curves reflect the  
501 system's overall trajectory (De'ath, 1999) and, as a form of indirect gradient analysis, PrC  
502 reflects the primary driver of the scenario. In contrast, FI is more sensitive to short-term  
503 variability (Eason et al., 2016) and so reflects driver interactions. Although FI does capture  
504 the long-term system trajectory, these trends can be obscured by short-term variability  
505 such as that caused by the random walk driver. Similar analyses (e.g., other ordination  
506 methods) may be affected by sources of uncertainty in similar ways. Of course, FI and PrC  
507 are only two of a suite of available statistical analyses (Birks et al., 2012; Blaauw et al.,  
508 2020), and an observer should apply more than one.

509 Alongside considerations of the sensitivity of analyses to uncertainty, there are questions of  
510 how sensitive different proxies are to driver change and, consequently, how informative  
511 the analyses are. The question of how different proxies respond to drivers at different  
512 temporal and spatial scales (e.g., Wilmshurst et al., 2002) remains poorly resolved.  
513 Interestingly, the sensitivity of different proxies to environmental change may be  
514 ecosystem-specific. Phytoliths have been reported as more sensitive than pollen to changes  
515 in dry forests, with the reverse being true of evergreen forests at a site in Bolivia  
516 (Plumpton et al., 2019). In savannahs, pollen and phytoliths are equally sensitive to  
517 changes in the environment (Plumpton et al., 2019). Thus, ecosystem-specific and proxy-  
518 specific knowledge are important considerations, as increasing sub-sampling efforts to  
519 obtain a higher resolution representation of change from numerical analyses may not be  
520 useful if the proxy is not a reliable sensor at that resolution. Furthermore, compositional  
521 change is not the sole (or necessarily the most appropriate) measure of system change, and  
522 other descriptors such as body-size distributions, physiognomic, and functional and  
523 phylogenetic diversity can be included (Adesanya Adeleye et al., 2023; Clements and Ozgul,  
524 2016; Goring et al., 2013; Reitalu et al., 2015; Spanbauer et al., 2016).

525

526 The advantage of using a phenomenological modelling approach designed to mimic the  
527 statistical properties of empirical data, is that the results are informative without  
528 attempting to recreate species abundances of a specific system and addressing the  
529 challenges faced by more process-based models. Our model and virtual approach can be  
530 used to assess, for example, the performance of statistical methods, the influence of  
531 observational and chronological uncertainty, and explore a range of driving environments.  
532 It becomes possible to address questions such as 'what statistical method is likely to be  
533 appropriate for my data and research question?' However, without recreating a specific  
534 system, it cannot answer questions such as 'should I use a 2 or 4 cm resolution sub-  
535 sampling procedure for this core?'. To answer such questions, process-based VE  
536 approaches are necessary. Of course, process-based models face numerous challenges of  
537 accurately representing mechanisms and being able to reasonably recreate a given system  
538 to address such questions. The VE approach can be applied using process-based models to  
539 generate data, or simulating data from a statistical model fit to the empirical data, and  
540 following the same process of degrading, sub-sampling and fitting/re-fitting, to assess how  
541 parameters change.

542 Finally, we can consider, empirical, experimental, semi-empirical approaches to advance  
543 our understanding of uncertainties in palaeoecology. Empirical approaches could involve  
544 collecting high-quality data (e.g., well-dated sediment cores with frequent sub-sampling  
545 resolution), ideally with replicate cores from the same location, to use as a benchmark  
546 against which to assess analyses when sub-sampling resolution is reduced (e.g., Liu et al.,  
547 2012). Experimental approaches might include laboratory and *in situ* manipulation; for  
548 example, Payne and Gehrels (2010) monitor the movement of tephra in the field and under  
549 controlled laboratory environments to understand the influence of tephra taphonomy on  
550 tephrochronology. Semi-empirical approaches would combining empirical-virtual methods  
551 could be developed using (virtually) modified empirical data; for example, applying a  
552 simulated mixing process to empirical sediment core data (such as those from varved  
553 sediments that are subject to minimal mixing) and assessing the subsequent analyses.  
554 Mann and Rutherford (2002) demonstrate this approach by generating pseudoproxy data  
555 by subjecting instrumental data to degradation, such as various noise processes and spatial  
556 sampling strategies, to assess sea surface temperature reconstruction methods. They used  
557 simulation to create a continuous sea surface temperature record from the patchier  
558 instrumental data before applying the degradation processes. Although the implications of  
559 such methods are different for ecological data, similar approaches could fruitfully be  
560 applied.

561

## 562 **5 Conclusion**

563 Palaeoecological uncertainty can be considered at four levels: environmental processes,  
564 field methods, laboratory methods, and quantitative analyses (Table 1). The effects of  
565 different sources of uncertainty are challenging to disentangle and quantify from empirical  
566 studies alone, and virtual ecology provides a useful approach as different uncertainties can  
567 be manipulated. However, virtual ecology has its own set of limitations. The data  
568 degradation and sampling processes described here still represent a relatively ideal  
569 situation in that the timespan of the data is long relative to the driving processes, and the  
570 sub-sampling treatment is at regular depth intervals for example. Thus, investigation of  
571 uncertainty through both empirical and virtual approaches is necessary to better  
572 understand the influence of process and observer error on the analysis of palaeoecological  
573 data. A better understanding of the how different proxies record environmental signals in  
574 an archive (e.g., how closely coupled a signal recorded by a proxy data is to the  
575 environmental change) and the uncertainties around quantifying and analysing proxy data  
576 can bring us closer to understanding long-term climate and ecosystem dynamics. Although  
577 we have assessed sources of uncertainty on pseudoproxy data representing species  
578 communities, all proxies such as isotopic data, or tree ring data, have their own  
579 idiosyncratic sources of uncertainty. Virtual Ecological approaches can help towards  
580 assessing their uncertainties.

581

582

583 **Acknowledgements**

584 The authors are very grateful for the support of the Centre for eResearch, University of  
585 Auckland particularly Nick Young and Noel Zeng for their digital research expertise. We  
586 also acknowledge the New Zealand eScience Infrastructure (NeSI) for the use of their  
587 computational resources, without which the scale of the analyses involved in this paper  
588 would not have been possible. Callum Walley and Anthony Shaw of NeSI provided  
589 instrumental support for high-performance computing. Finally, we extend our thanks to  
590 members of the Perry Lab for helping shape the project.

591 **Data availability**

592 Functions used to compute Fisher Information and the derived metrics can be found here:  
593 <https://doi.org/10.5281/zenodo.8052806>. Additional functions used to calculate metrics  
594 from principal curves can be found here: <https://doi.org/10.5281/zenodo.18200665>.

595

596 **Author contributions**

597 QA contributed to the conceptualization, methodology, and writing the original draft. GLWP  
598 contributed to the conceptualization, methodology, and reviewing and editing the  
599 manuscript, providing supervision and statistical expertise. JMW provided palaeoecological  
600 expertise to the project, and reviewed and edited the manuscript.

601

602 **Competing interests**

603 The authors declare that they have no conflict of interest.

604

605 **Funding**

606 The author(s) disclosed receipt of the following financial support for the research,  
607 authorship, and/or publication of this article: This work was conducted through the New  
608 Zealand's Biological Heritage National Science Challenge, which is funded by the New  
609 Zealand Ministry of Business, Innovation and Employment.

610

611 **References**

612 Adesanya Adeleye, M., Charles Andrew, S., Gallagher, R., van der Kaars, S., De Deckker, P.,  
613 Hua, Q., and Haberle, S. G.: On the timing of megafaunal extinction and associated floristic  
614 consequences in Australia through the lens of functional palaeoecology, *Quat. Sci. Rev.*, 316,  
615 108263, <https://doi.org/10.1016/j.quascirev.2023.108263>, 2023.

616 Asena, Q., Young, N., and Pletzer, A.: UoA-eResearch/fisheR: v1.0.0,  
617 <https://doi.org/10.5281/ZENODO.8052806>, 2023.

618 Asena, Q., Perry, G. L., and Wilmshurst, J. M.: Is the past recoverable from the data?  
619 Pseudoproxy modelling of uncertainties in palaeoecological data, *The Holocene*,  
620 09596836241247304, 2024.

621 Benito, B. M., Gil-Romera, G., and Birks, H. J. B.: Ecological Memory at Millennial Time-  
622 Scales: The Importance of Data Constraints, Species Longevity and Niche Features,  
623 *Ecography*, 43, 1–10, <https://doi.org/10.1111/ecog.04772>, 2020.

624 Birks, J. B. H., Lotter, A. F., Juggins, S., and Smol, J. P.: Tracking environmental change using  
625 lake sediments: data handling and numerical techniques, Springer Science & Business  
626 Media, 751 pp., 2012.

627 Blaauw, M.: Out of tune: the dangers of aligning proxy archives, *Quat. Sci. Rev.*, 36, 38–49,  
628 <https://doi.org/10.1016/j.quascirev.2010.11.012>, 2012.

629 Blaauw, M., Bennett, K. D., and Christen, J. A.: Random walk simulations of fossil proxy data,  
630 *The Holocene*, 20, 645–649, <https://doi.org/10.1177/0959683609355180>, 2010.

631 Blaauw, M., Christen, J. A., Bennett, K. D., and Reimer, P. J.: Double the dates and go for  
632 Bayes - Impacts of model choice, dating density and quality on chronologies, *Quat. Sci. Rev.*,  
633 188, 58–66, <https://doi.org/10.1016/J.QUASCIREV.2018.03.032>, 2018.

634 Blaauw, M., Christen, J. A., and Aquino-López, M. A.: A review of statistics in  
635 palaeoenvironmental research, *J. Agric. Biol. Environ. Stat.*, 25, 17–31,  
636 <https://doi.org/10.1007/s13253-019-00374-2>, 2020.

637 Bothe, O., Wagner, S., and Zorita, E.: Simple noise estimates and pseudoproxies for the last  
638 21000 years, *Earth Syst. Sci. Data*, 11, 1129–1152, [https://doi.org/10.5194/essd-11-1129-](https://doi.org/10.5194/essd-11-1129-2019)  
639 2019, 2019.

640 Cabezas, H. and Fath, B. D.: Towards a theory of sustainable systems, *Fluid Phase Equilibria*,  
641 194–197, 3–14, [https://doi.org/10.1016/S0378-3812\(01\)00677-X](https://doi.org/10.1016/S0378-3812(01)00677-X), 2002.

642 Christiansen, B., Schmith, T., and Thejll, P.: A surrogate ensemble study of climate  
643 reconstruction methods: Stochasticity and robustness, *J. Clim.*, 22, 951–976,  
644 <https://doi.org/10.1175/2008JCLI2301.1>, 2009.

645 Clements, C. F. and Ozgul, A.: Including trait-based early warning signals helps predict  
646 population collapse, *Nat. Commun.*, 7, <https://doi.org/10.1038/ncomms10984>, 2016.

647 De'ath, G.: Principal curves: a new technique for indirect and direct gradient analysis,  
648 *Ecology*, 80, 2237–2253, [https://doi.org/10.1890/0012-](https://doi.org/10.1890/0012-9658(1999)080%255B2237:PCANTF%255D2.0.CO;2)  
649 9658(1999)080%255B2237:PCANTF%255D2.0.CO;2, 1999.

- 650 Dormann, C. F., McPherson, J. M., Araújo, M. B., Bivand, R., Bolliger, J., Carl, G., Davies, R. G.,  
651 Hirzel, A., Jetz, W., Kissling, W. D., Kühn, I., Ohlemüller, R., Peres-Neto, P. R., Reineking, B.,  
652 Schröder, B., Schurr, F. M., and Wilson, R.: Methods to Account for Spatial Autocorrelation in  
653 the Analysis of Species Distributional Data: A Review, *Ecography*, 30, 609–628,  
654 <https://doi.org/10.1111/j.2007.0906-7590.05171.x>, 2007.
- 655 Eason, T. and Cabezas, H.: Evaluating the Sustainability of a Regional System Using Fisher  
656 Information in the San Luis Basin, Colorado, *J. Environ. Manage.*, 94, 41–49,  
657 <https://doi.org/10.1016/j.jenvman.2011.08.003>, 2012.
- 658 Eason, T., Garmestani, A. S., Stow, C. A., Rojo, C., Alvarez-Cobelas, M., and Cabezas, H.:  
659 Managing for resilience: an information theory-based approach to assessing ecosystems, *J.*  
660 *Appl. Ecol.*, 53, 656–665, <https://doi.org/10.1111/1365-2664.12597>, 2016.
- 661 Evans, M. N., Tolwinski-Ward, S. E., Thompson, D. M., and Anchukaitis, K. J.: Applications of  
662 proxy system modeling in high resolution paleoclimatology, *Quat. Sci. Rev.*, 76, 16–28,  
663 <https://doi.org/10.1016/j.quascirev.2013.05.024>, 2013.
- 664 Fisher, R. A.: On the Mathematical Foundations of Theoretical Statistics, *Philos. Trans. R.*  
665 *Soc. Lond. Ser. Contain. Pap. Math. Phys. Character*, 222, 309–368, 1922.
- 666 Goring, S., Lacourse, T., Pellatt, M. G., and Mathewes, R. W.: Pollen assemblage richness does  
667 not reflect regional plant species richness: a cautionary tale, *J. Ecol.*, 101, 1137–1145,  
668 <https://doi.org/10.1111/1365-2745.12135>, 2013.
- 669 Hastie, T. and Stuetzle, W.: Principal curves, *J. Am. Stat. Assoc.*, 84, 502–516,  
670 <https://doi.org/10.1080/01621459.1989.10478797>, 1989.
- 671 Jackson, S. T.: Looking forward from the past: history, ecology, and conservation, *Front.*  
672 *Ecol. Environ.*, 5, 455–455, [https://doi.org/10.1890/1540-9295\(2007\)5%255B455:LFFTPH%255D2.0.CO;2](https://doi.org/10.1890/1540-9295(2007)5%255B455:LFFTPH%255D2.0.CO;2), 2007.
- 674 Karunanithi, A. T., Cabezas, H., Frieden, B. R., and Pawlowski, C. W.: Detection and  
675 assessment of ecosystem regime shifts from Fisher information, *Ecol. Soc.*, 13, 2008.
- 676 Killick, R. and Eckley, I. A.: Changepoint: An r Package for Changepoint Analysis, *J. Stat.*  
677 *Softw.*, 58, 1–19, <https://doi.org/10.18637/jss.v058.i03>, 2014.
- 678 Kim, D.-W., Protopapas, P., Byun, Y.-I., Alcock, C., Khardon, R., and Trichas, M.: Quasi-Stellar  
679 Object Selection Algorithm Using Time Variability and Machine Learning: Selection of 1620  
680 Quasi-Stellar Object Candidates from Macho Large Magellanic Cloud Database, *Astrophys.*  
681 *J.*, 735, 68, <https://doi.org/10.1088/0004-637X/735/2/68>, 2011.
- 682 Kosnik, M. A. and Kowalewski, M.: Understanding modern extinctions in marine  
683 ecosystems: the role of palaeoecological data, *Biol. Lett.*, 12,  
684 <https://doi.org/10.1098/rsbl.2015.0951>, 2016.

685 Liu, Y., Brewer, S., Booth, R. K., Minckley, T. A., and Jackson, S. T.: Temporal density of pollen  
686 sampling affects age determination of the mid-Holocene hemlock (*Tsuga*) decline, *Quat. Sci.*  
687 *Rev.*, 45, 54–59, <https://doi.org/10.1016/j.quascirev.2012.05.001>, 2012.

688 Mann, M. E. and Rutherford, S.: Climate reconstruction using ‘Pseudoproxies,’ *Geophys. Res.*  
689 *Lett.*, 29, 139-1-139-4, <https://doi.org/10.1029/2001GL014554>, 2002.

690 Mayer, A. L., Pawlowski, C. W., and Cabezas, H.: Fisher Information and dynamic regime  
691 changes in ecological systems, *Ecol. Model.*, 195, 72–82,  
692 <https://doi.org/10.1016/j.ecolmodel.2005.11.011>, 2006.

693 Nun, I., Protopapas, P., Sim, B., Zhu, M., Dave, R., Castro, N., and Pichara, K.: FATS: Feature  
694 analysis for time series, arXiv:1506.00010, 2015.

695 Parnell, A. C., Haslett, J., Allen, J. R. M., Buck, C. E., and Huntley, B.: A flexible approach to  
696 assessing synchronicity of past events using Bayesian reconstructions of sedimentation  
697 history, *Quat. Sci. Rev.*, 27, 1872–1885, <https://doi.org/10.1016/j.quascirev.2008.07.009>,  
698 2008.

699 Payne, R. and Gehrels, M.: The formation of tephra layers in peatlands: An experimental  
700 approach, *CATENA*, 81, 12–23, <https://doi.org/10.1016/j.catena.2009.12.001>, 2010.

701 Peck, S. L.: Simulation as experiment: a philosophical reassessment for biological modeling,  
702 *Trends Ecol. Evol.*, 19, 530–534, <https://doi.org/10.1016/j.tree.2004.07.019>, 2004.

703 Plumpton, H., Whitney, B., and Mayle, F.: Ecosystem turnover in palaeoecological records:  
704 The sensitivity of pollen and phytolith proxies to detecting vegetation change in  
705 southwestern Amazonia: The Holocene, 29, 1720–1730,  
706 <https://doi.org/10.1177/0959683619862021>, 2019.

707 R Core Team: R: a language and environment for statistical computing. Version 4.0.1, 2020.

708 Reitalu, T., Gerhold, P., Poska, A., Pärtel, M., Väli, V., and Veski, S.: Novel insights into post-  
709 glacial vegetation change: functional and phylogenetic diversity in pollen records, *J. Veg.*  
710 *Sci.*, 26, 911–922, <https://doi.org/10.1111/jvs.12300>, 2015.

711 Richards, J. W., Starr, D. L., Butler, N. R., Bloom, J. S., Brewer, J. M., Crellin-Quick, A., Higgins,  
712 J., Kennedy, R., and Rischard, M.: On Machine-Learned Classification of Variable Stars with  
713 Sparse and Noisy Time-Series Data, *Astrophys. J.*, 733, 10, [https://doi.org/10.1088/0004-  
714 637X/733/1/10](https://doi.org/10.1088/0004-637X/733/1/10), 2011.

715 Roberts, C. P., Twidwell, D., Burnett, J. L., Donovan, V. M., Wonkka, C. L., Bielski, C. L.,  
716 Garmestani, A. S., Angeler, D. G., Eason, T., Allred, B. W., Jones, M. O., Naugle, D. E.,  
717 Sundstrom, S. M., and Allen, C. R.: Early Warnings for State Transitions, *Rangel. Ecol.*  
718 *Manag.*, 71, 659–670, <https://doi.org/10.1016/j.rama.2018.04.012>, 2018.

- 719 Simpson, G. L.: Analogue methods in palaeolimnology, edited by: Birks, H. J. B., Lotter, A. F.,  
720 Juggins, S., and Smol, J. P., *Track. Environ. Change Using Lake Sediments 5 Data Handl.*  
721 *Numer. Tech.*, 249–327, 2012.
- 722 Simpson, G. L. and Oksanen, J.: Analogue matching and Modern Analogue Technique  
723 transfer function models. Version 0.17-4, 2020.
- 724 Smerdon, J. E.: Climate models as a test bed for climate reconstruction methods:  
725 pseudoproxy experiments, *WIREs Clim. Change*, 3, 63–77,  
726 <https://doi.org/10.1002/wcc.149>, 2012.
- 727 Sokolovsky, K. V., Gavras, P., Karampelas, A., Antipin, S. V., Bellas-Velidis, I., Benni, P.,  
728 Bonanos, A. Z., Burdanov, A. Y., Derlopa, S., Hatzidimitriou, D., Khokhryakova, A. D.,  
729 Kolesnikova, D. M., Korotkiy, S. A., Lapukhin, E. G., Moretti, M. I., Popov, A. A., Pouliasis, E.,  
730 Samus, N. N., Spetsieri, Z., Veselkov, S. A., Volkov, K. V., Yang, M., and Zubareva, A. M.:  
731 Comparative Performance of Selected Variability Detection Techniques in Photometric  
732 Time Series, *Mon. Not. R. Astron. Soc.*, 464, 274–292,  
733 <https://doi.org/10.1093/mnras/stw2262>, 2017.
- 734 Spanbauer, T. L., Allen, C. R., Angeler, D. G., Eason, T., Fritz, S. C., Garmestani, A. S., Nash, K.  
735 L., and Stone, J. R.: Prolonged instability prior to a regime shift, *PLoS ONE*, 9,  
736 <https://doi.org/10.1371/journal.pone.0108936>, 2014.
- 737 Spanbauer, T. L., Allen, C. R., Angeler, D. G., Eason, T., Fritz, S. C., Garmestani, A. S., Nash, K.  
738 L., Stone, J. R., Stow, C. A., and Sundstrom, S. M.: Body size distributions signal a regime shift  
739 in a lake ecosystem, *Proc. R. Soc. B Biol. Sci.*, 283, <https://doi.org/10.1098/rspb.2016.0249>,  
740 2016.
- 741 Taranu, Z. E., Carpenter, S. R., Frossard, V., Jenny, J.-P., Thomas, Z., Vermaire, J. C., and Perga,  
742 M.-E.: Can we detect ecosystem critical transitions and signals of changing resilience from  
743 paleo-ecological records?, *Ecosphere*, 9, <https://doi.org/10.1002/ecs2.2438>, 2018.
- 744 Telford, R. J., Heegaard, E., and Birks, H. J. B.: All age-depth models are wrong: but how  
745 badly?, *Quat. Sci. Rev.*, 23, 1–5, <https://doi.org/10.1016/J.QUASCIREV.2003.11.003>, 2004.
- 746 Williams, J. W., Blois, J. L., and Shuman, B. N.: Extrinsic and intrinsic forcing of abrupt  
747 ecological change: case studies from the late Quaternary, *J. Ecol.*, 99, 664–677,  
748 <https://doi.org/10.1111/j.1365-2745.2011.01810.x>, 2011.
- 749 Wilmshurst, J. M., McGlone, M. S., and Charman, D. J.: Holocene vegetation and climate  
750 change in southern New Zealand: linkages between forest composition and quantitative  
751 surface moisture reconstructions from an ombrogenous bog, *J. Quat. Sci.*, 17, 653–666,  
752 <https://doi.org/10.1002/jqs.689>, 2002.
- 753 Zurell, D., Berger, U., Cabral, J. S., Jeltsch, F., Meynard, C. N., Münkemüller, T., Nehrbass, N.,  
754 Pagel, J., Reineking, B., Schröder, B., and Grimm, V.: The virtual ecologist approach:

755 simulating data and observers, *Oikos*, 119, 622–635, <https://doi.org/10.1111/j.1600->  
756 0706.2009.18284.x, 2010.

757